Ultrafast FBG Interrogator Based on Time-Stretch Method

Meng Lei, Weiwen Zou, *Senior Member, IEEE*, Xing Li, and Jianping Chen

***Abstract*— We demonstrate an experimental realization of the time-stretch configured fiber Bragg grating (FBG) interrogator with an ultrafast speed. The interrogator consists of a home-made ultrabroadband fiber laser, an FBG sensor array, and two dispersive elements (single mode fibers). A time-stretch method is employed to convert the wavelength shift of the FBG sensor array to time shift via the principle of wavelength-to-time mapping. It is theoretically and experimentally demonstrated that the wavelength-related time shift suffers no influence although the Bragg wavelength and bandwidth of the strained FBG might be different. The interrogator works in real time, so that a single-shot measurement without carrying out any averaging is feasible.**

***Index Terms*— Time stretch, fiber Bragg grating (FBG), wavelength-to-time mapping, mode-locked laser (MLL).**

I. Introduction

FBG-BASED optical sensors have been extensively investigated and developed in last decades. They offer many advantages of small size, low cost, multipoint sensing capability, high resistance to chemical corrosion, and immunity to electromagnetic interference. Therefore, they have been widely adopted to the monitoring of strain, temperature, mechanical, chemical, and biomedical parameters in smart structures, civil engineering, or other harsh environments [1]–[3]. Most of the FBG sensors are based on wavelength modulation, in which the sensing information of strain or temperature variation is directly encoded as the grating wavelength change. The conventional interrogation techniques can be generally classified into two main types depending on the detection method. The first type is implemented by non-interferometric scheme, for which a static frequency discriminator is used to convert the wavelength shift of an FBG signal into an intensity change. It can be realized by using an optical edge filter [4], [5], an arrayed waveguide grating [6], [7], a wavelength-division-multiplexed (WDM) fiber coupler [8], or a holographic grating-based spectroscopic charge-coupled device (CCD) [9]–[11]. The advantage of non-interferometric scheme is that the system is simple and cost-effective. However, the power fluctuation from the light source or environmental disturbance is transferred to the detector's output signal and limits the resolution. The second type is realized by interferometric scheme. The wavelength shift in the FBG sensor is converted into the phase change of the received signal. The interference structure can be an unbalanced Mach-Zehnder interferometer (MZI) [12], a Fabry-Perot interferometer [13]–[15], a Michelson interferometer [16], [17], or a long-period fiber grating (LPG) pair interferometer [18]. The measurement resolution of interferometric scheme is much higher compared with non-interferometric scheme due to elimination of power fluctuations. However, an interferometric scheme is sensitive to environmental disturbances, such as temperature change or subtle vibration, which would obviously deteriorate the system stability. In addition, the speed of interrogation system employing interferometric scheme is limited to a few kilohertz and the dynamic range of a few nanometers is still small [12]–[18].

However, interrogation of FBG sensors with a speed up to hundreds of megasamples per second is desirable in many applications such as molecular dynamics sensing and aerospace diagnostics. In order to obtain high-speed, high resolution, and large dynamic range interrogation of multiple FBG sensor system, the mode-locked fiber laser has been proposed as a pulsed optical source [19]–[24]. M. L. Dennis *et al.* firstly proposed a novel method to map the power spectrum of an ultrashort pulse to a temporal waveform via an optical dispersive element, which can be recorded and processed by a high-speed real-time oscilloscope [19]. Furthermore, the pulsed nature of the optical sensing signal enables an ultrafast and single-short measurement. However, in the aforementioned systems [19], [21]–[24], the output characteristics of the pulsed laser severely limit the interrogation speed and dynamic range.

In this letter, we demonstrate an ultrahigh-speed multiplexed FBG sensor interrogation using a homemade broadband passive mode-locked fiber laser. Two dispersion modules are used to map wavelength to time under a time-stretch scheme. The output from the mode-locked fiber laser is coupled into the multiplexed FBG array which consists of five FBGs with different Bragg wavelengths. Two of the multiplexed FBGs in the array are fixed on the stage of the piezoelectric transducer (PZT) to apply the tensile strain. Time-stretch method is employed to stretch the pulse in time, so that the interrogation accuracy can be significantly increased.

II. Principle and Experimental Setup

Figure 1 shows the operating principle of the proposed FBG interrogator based on the time-stretch scheme. It includes

Manuscript received August 19, 2015; revised December 3, 2015; accepted December 29, 2015. Date of publication December 31, 2015; date of current version February 25, 2016. This work was supported in part by the National Natural Science Foundation of China under Grant 61535006 and Grant 61571292, in part by the Specialized Research Fund within the Doctoral Program through the Ministry of Education under Grant 20130073130005, in part by the State Key Laboratory Project of Shanghai Jiao Tong University under Grant 2014ZZ03016, and in part by Shanghai Key Laboratory of Specialty Fiber Optics and Optical Access Networks under Grant SKLSFO2015-04. *(Corresponding author: Weiwen Zou.)*

The authors are with the State Key Laboratory of Advanced Optical Communication Systems and Networks, Shanghai Jiao Tong University, Shanghai 200240, China (e-mail: doreendavis@sjtu.edu.cn; wzou@sjtu.edu.cn; lixing85715@sjtu.edu.cn; jpchen62@sjtu.edu.cn).

Color versions of one or more of the figures in this letter are available online at http://ieeexplore.ieee.org.

Digital Object Identifier 10.1109/LPT.2015.2513903

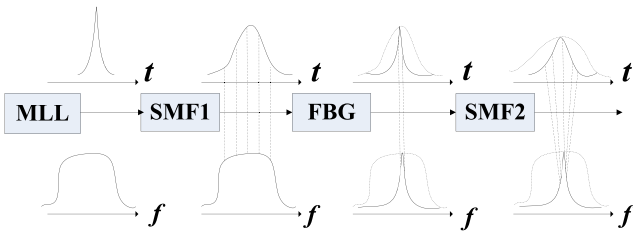

Fig. 1. Principle of the time-stretch based multiple FBG sensing interrogator. MLL: mode-locked laser. SMF: single mode fiber. FBG: fiber Bragg grating.

a mode-locked laser, two group velocity dispersion (GVD) elements (such as single mode fibers, SMFs), and a FBG sensor array. The ultrashort optical pulse produced by the MLL is temporally chirped through the first SMF1 with length L_1 and GVD value of D_1. This process results in time-to-wavelength mapping in the stretched pulse since different wavelength components travel at different GVD. After reflected by the FBG sensor, the reflected pulse, carrying the sensing information of the Bragg wavelength shift, is then stretched in the second SMF2 with length L_2 and GVD value of D_2. The upper side shows the time-domain profile after each element and the lower side shows the corresponding spectrum.

At the input of FBG, the pulse width in the time domain (t_{in}) is determined by:

$$t_{in} = \Delta\lambda \times D_1, \tag{1}$$

At the output of SMF2, the pulse width in the time domain (t_{out}) is given by:

$$t_{out} = \Delta\lambda \times (D_1 + D_2), \tag{2}$$

where $\Delta\lambda$ is the spectral bandwidth of the pulse. The wavelength resolution ($\delta\lambda_0$) can be deduced as follows:

$$\delta\lambda_0 = \delta t_0 / (D_1 + D_2), \tag{3}$$

where δt_0 is the time resolution of the data recording device. Although this work utilizes the time-stretch configuration, $\delta\lambda_0$ is determined by the total GVD of dispersive elements, which is the same as the previous configurations based on the wavelength-to-time mapping principle [19]–[24].

If the same dispersive medium of single mode fibers (SMFs) are used, the time-stretch factor is given by [25]

$$M = \frac{t_{out}}{t_{in}} = \frac{D_1 + D_2}{D_1} = \frac{L_1 + L_2}{L_1} \tag{4}$$

Consider that two FBGs suffer different strains and have different reflected Bragg wavelength of λ_1 and λ_2. Without loss of generality, we assume that the reflected pulses from the two FBGs have the same pulse duration of δt since they might have different bandwidths of $\delta\lambda_1$ and $\delta\lambda_2$, respectively. In mathematics,

$$\delta \mathrm{t} = \delta\lambda_1 \times D_{11} = \delta\lambda_2 \times D_{12} \tag{5}$$

where D_{11} and D_{12} is the dispersion of SMF1 corresponding to λ_1 and λ_2. After propagating through SMF2, the reflected pulses are respectively stretched to

$$\delta t_1 = \delta\lambda_1 \times (D_{11} + D_{21}) \tag{6}$$

$$\delta t_2 = \delta\lambda_2 \times (D_{12} + D_{22}) \tag{7}$$

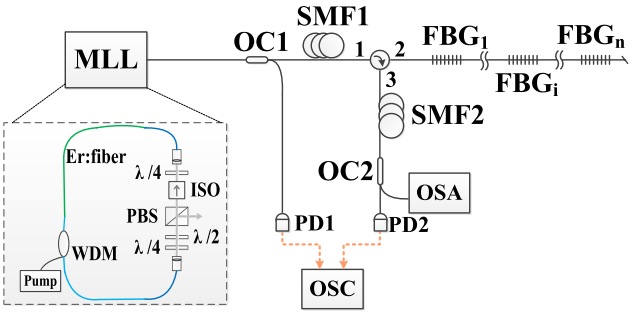

Fig. 2. Experimental setup of the time-stretch based FBG interrogation system. OC: optical coupler. PD: photodetector. OSA: optical spectrum analyzer. OSC: oscilloscope.

where D_{21} and D_{22} is the dispersion of SMF2 corresponding to λ_1 and λ_2. There's a basic relationship that $\frac{D_{22}}{D_{12}} = \frac{D_{21}}{D_{11}} = \frac{L_2}{L_1}$, although $D_{11} \neq D_{12}$ and $D_{21} \neq D_{22}$. Substituting Eq. (5) into Eqs. (6-7), we get

$$\delta t_1 = \delta t_2 \tag{8}$$

which means that the reflected pulses of the two different FBGs have the same durations since they are stretched by the same time-stretch factor of M defined in Eq. (4). Moreover, it indicates that the wavelength-to-time mapping works equally despite of the different Bragg wavelength and bandwidth of the strained FBGs.

Figure 2 shows an experimental setup of the FBG array sensing system which consists of a home-made passive mode-locked fiber laser (MLL), an optical circulator, two optical coupler (OC1, 99:1 and OC2, 50:50), and two single mode fibers SMF1 and SMF2 (SMF28) with an anomalous GVD of -22 fs^2/mm The fiber laser employed in this work is a typical passively mode-locked ring fiber laser based on nonlinear polarization rotation (NPR). Dispersion and nonlinearity management is applied and the net GVD of the laser cavity is managed to near-zero at 1550 nm so that the fiber laser can generate ultrashort pulse with broad spectrum [26]. Fundamental mode-locking with a repetition frequency of 201.64 MHz (see Fig. 3(a)) is achieved by adjusting the wave plates at a pump power of 700 mW. The signal-to-background ratio of the fundamental frequency is up to 85 dB at a resolution bandwidth of 300 Hz (see Fig. 3(b)). After optimizing the polarization state existing in the cavity, a broad spectrum with a full width at half magnitude (FWHM) of 84.2 nm is achieved (see Fig. 3(c)). As shown in Fig. 3(d), the direct output pulse is 91.6 fs with an average output power of 50.2 mW.

The output pulse from the fiber laser is split into two branches by OC1. The first branch (1% output) is detected by a 1 GHz photodetector (PD1) and measured by an oscilloscope (OSC). The second branch (99% output) is launched into the SMF1 with a short length and fed into the multiplexed FBG array through a circulator. The FBG array consists of five FBGs with different Bragg wavelengths (1545 nm, 1550 nm, 1558 nm, 1567 nm, and 1575 nm, respectively). The FBG3 and FBG4 are glued on a stage of PZT for strain loading and three other FBG sensors are used as reference. Therefore, the influence of temperature fluctuation is cancellable as we

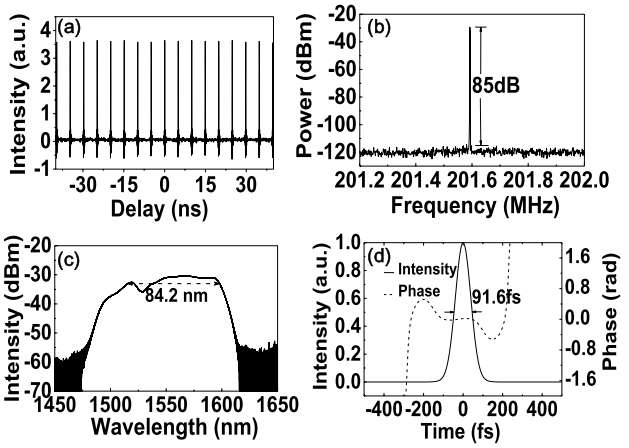

Fig. 3. Characteristics of the home-made passive mode-locked laser. (a) Pulse train, (b) fundamental RF spectrum, (c) optical spectrum, and (d) temporal profile.

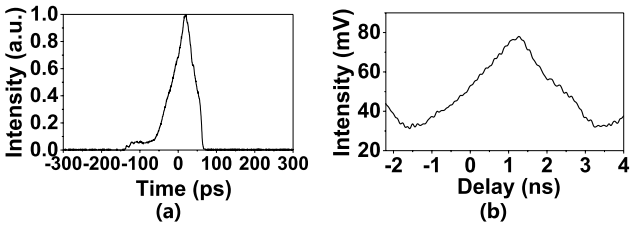

Fig. 4. Time-domain profile of the pulse after (a) SMF1 and (b) SMF2.

measure the relative time shift between the two pulses reflected by a sensing FBG and a reference FBG. The temporal and spectral interferogram are recorded using an oscilloscope and an optical spectrum analyzer (OSA), respectively. A part of the optical pulse which falls in the reflection spectrum of the FBG array is reflected back to the circulator and launched into the SMF2 with a long length. The pulse reflected by the FBG array corresponds to different spectral components. Therefore, different GVD after the SMF2 is accumulated for the FBG array so that both the bandwidths of the PD and the OSC are significantly reduced because of the time-stretch effect.

III. Results and Discussion

The time shape of laser after the two dispersive elements is shown in Fig. 4. Figure 4(a) denotes the time shape of the pulse after SMF1 with a duration of 40.64 ps, which is measured by an autocorrelator (Femtochrome, FR-103XL). The pulse is stretched to 1.85 ns by SMF2, as shown in Fig. 4(b). Note that Fig. 4(b) is measured by two steps: opto-electronic conversion by a PD (EOT, ET-3500F) and recording by an 8 GHz oscilloscope (Tektronix DSA70804). So the actual time-stretch factor defined in Eq. (3) is M = 45.5.

The reflection spectra of the FBG array under different applied strains are measured by the optical spectrum analyzer (OSA). Figure 5(a) or 5(b) corresponds to two different cases: only SMF1 is used; both SMF1 and SMF2 are employed. Both cases show clear wavelength shifts of FBG3 and FBG4 at 1558 nm and 1567 nm. There is only power difference due to the transmission and insertion loss of the SMF2. Figure 5(c) shows the wavelength shift when different strains are applied. The wavelength-strain sensitivity

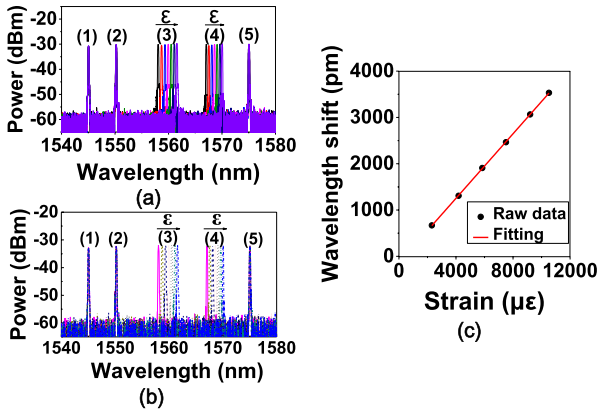

Fig. 5. Reflection spectra of the FBG array after (a) SMF1 and (b) SMF2. (c) Wavelength shift as a function of the applied strain.

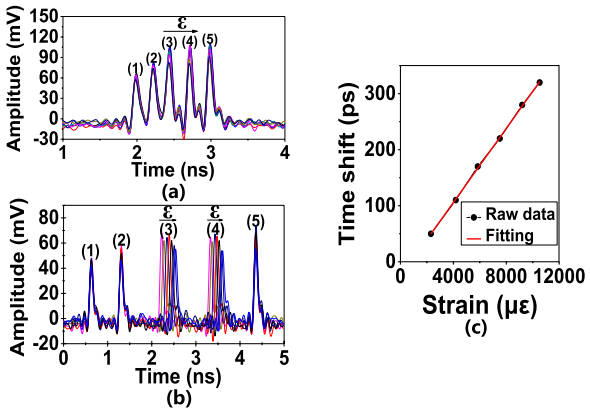

Fig. 6. Time-domain profile of the FBG array after (a) SMF1 and (b) SMF2. (c) Time shift as a function of the applied strain.

of the FBG is measured to be 0.35 pm/$\mu\varepsilon$, which is smaller than the typical value of 1.2 pm/$\mu\varepsilon$ [22]. This is possibly due to the loose jackets of the FBGs used in the experiment so that the effective strain is released to some extent.

Owing to the wavelength-to-time mapping effect of SMFs, the wavelength shift of the FBGs is mapped to time shift that can be directly measured by the oscilloscope. Figure 6(a) shows the time-domain profiles of the FBG array in one period when only SMF1 is used. Note that under this condition, the time shift is almost overlapped and unable to correctly distinguish. When the SMF2 is additionally employed, the time spacing is stretched significantly. As depicted in Fig. 6(b), the third and fourth pulses of the same period clearly identify the time shift of the FBG3 and FBG4, respectively. When the applied strain is increased, the Bragg wavelength shifts right (see Fig. 5(b)) and the corresponding pulse in time domain also shifts right (see Fig. 6(b)). Figure 6(c) shows the time shift as a function of the applied strain with a good linear slope of 0.033 ps/$\mu\varepsilon$. Note that the time-stretch factors calculated for all FBGs, i.e., division of the pulse durations shown in Fig. 6(b) and Fig. 6(a), is always equal to each other and also to that deduced from Fig. 4.

Figure 7 summarizes the measured time shift against the measured wavelength shift for both strained FBGs (FBG3 and FBG4). The Bragg wavelength of the FBGs within the range of 50 nm are linearly varied with respect to the

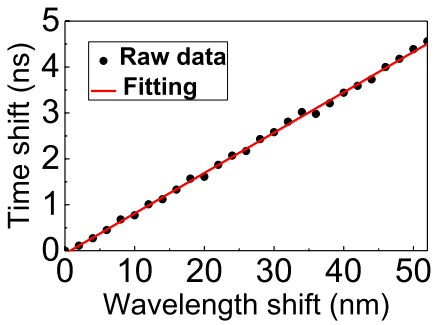

Fig. 7. Measured time shift as a function of the wavelength shift when different strain is applied.

time shift. The results further demonstrate that the mapping of wavelength shift to time shift suffers no influence from the different Bragg wavelength and bandwidth of the strained FBGs. It experimentally verifies the feasibility of Eq. (8). The coefficient of time shift against wavelength shift is deduced to be 0.088 ns/nm for both FBGs, which is in principle determined by the total GVD of dispersive elements [see Eq. (2)]. The OSC used in this study has a time resolution of $\delta t_0 = 40$ ps, which corresponds to the wavelength resolution is $\delta\lambda_0 = 454.5$ pm. It's undergoing to improve $\delta\lambda_0$ by adopting a higher performance oscilloscope [21] as well as a larger time-stretch factor with greater total GVD.

IV. Conclusion

An ultrafast FBG interrogation system based on time-stretch method has been demonstrated. By using a home-made broadband passive mode-locked fiber laser with a repetition frequency of 201 MHz and a broad spectrum of 84.2 nm, the sensing system can operate with large dynamic range at ultrafast speed. The pulse is stretched in time by using two SMFs. The larger the time stretch factor, the wider the stretched pulse. We also demonstrate that the wavelength-related time shift isn't influenced by the Bragg wavelength and bandwidth of the FBGs. Besides, the interrogation speed is identical to the repetition rate of the MLL due to the single-shot data recording. In the further experiment, we will apply a high-frequency dynamic strain to verify the ultrafast speed (201 MHz) of the FBG interrogation system. Moreover, the maximum dynamic range can be increased and more FBG sensors can be interrogated when a much broader MLL [27] is used and a higher interrogation resolution is expectable when a higher performance OSC is employed.

References

[1] A. Kersey *et al.*, "Fiber grating sensors," *J. Lightw. Technol.*, vol. 15, no. 8, pp. 1442–1463, Aug. 1997.
[2] Y.-J. Rao, "In-fibre Bragg grating sensor," *Meas. Sci. Technol.*, vol. 8, no. 4, pp. 355–375, Apr. 1997.
[3] A. Othonos, "Fiber Bragg gratings," *Rev. Sci. Instrum.*, vol. 68, no. 12, pp. 4309–4341, Dec. 1997.
[4] S. M. Melle, K. Liu, and R. M. Measures, "A passive wavelength demodulation system for guided-wave Bragg grating sensors," *IEEE Photon. Technol. Lett.*, vol. 4, no. 5, pp. 516–518, May 1992.
[5] Q. Zhang *et al.*, "Use of highly overcoupled couplers to detect shifts in Bragg wavelength [strain sensors]," *Electron. Lett.*, vol. 31, no. 6, pp. 480–482, Mar. 1995.
[6] A. Fender *et al.*, "Dynamic two-axis curvature measurement using multicore fiber Bragg gratings interrogated by arrayed waveguide gratings," *Appl. Opt.*, vol. 45, no. 36, pp. 9041–9048, Dec. 2006.
[7] Y. Sano and T. Yoshino, "Fast optical wavelength interrogator employing arrayed waveguide grating for distributed fiber Bragg grating sensors," *J. Lightw. Technol.*, vol. 21, no. 1, pp. 132–139, Jan. 2003.
[8] M. A. Davis and A. D. Kersey, "All-fibre Bragg grating strain-sensor demodulation technique using a wavelength division coupler," *Electron. Lett.*, vol. 30, no. 1, pp. 75–76, Jan. 1994.
[9] C. G. Askins, M. A. Putnam, G. M. Williams, and E. J. Friebele, "Stepped-wavelength optical fiber Bragg grating arrays fabricated in line on a draw tower," *Opt. Lett.*, vol. 19, no. 2, pp. 147–149, Jan. 1994.
[10] W. Ecke, I. Latka, R. Willsch, A. Reutlinger, and R. Graue, "Fibre optic sensor network for spacecraft health monitoring," *Meas. Sci. Technol.*, vol. 12, no. 7, pp. 974–980, Jul. 2001.
[11] K. Zhou, A. G. Simpson, X. Chen, L. Zhang, and I. Bennion, "Fiber Bragg grating sensor interrogation system using a CCD side detection method with superimposed blazed gratings," *IEEE Photon. Technol. Lett.*, vol. 16, no. 6, pp. 1549–1551, Jun. 2004.
[12] A. D. Kersey and T. A. Berkoff, "Fiber-optic Bragg-grating differential-temperature sensor," *IEEE Photon. Technol. Lett.*, vol. 4, no. 10, pp. 1183–1185, Oct. 1992.
[13] H. Xia, C. Zhang, H. Mu, and D. Sun, "Edge technique for direct detection of strain and temperature based on optical time domain reflectometry," *Appl. Opt.*, vol. 48, no. 2, pp. 189–197, Jan. 2009.
[14] A. D. Kersey, T. A. Berkoff, and W. W. Morey, "Multiplexed fiber Bragg grating strain-sensor system with a fiber Fabry–Perot wavelength filter," *Opt. Lett.*, vol. 18, no. 16, pp. 1370–1372, Aug. 1993.
[15] K. V. Madhav and S. Asokan, "Spectrum estimation by wavelength shift time-stamping in a fiber Bragg grating sensor," *IEEE Photon. Technol. Lett.*, vol. 16, no. 5, pp. 1355–1357, May 2004.
[16] Y. J. Rao, D. A. Jackson, L. Zhang, and I. Bennion, "Dual-cavity interferometric wavelength-shift detection for in-fiber Bragg grating sensors," *Opt. Lett.*, vol. 21, no. 19, pp. 1556–1558, Oct. 1996.
[17] M. A. Davis and A. D. Kersey, "Application of a fiber Fourier transform spectrometer to the detection of wavelength-encoded signals from Bragg grating sensors," *J. Lightw. Technol.*, vol. 13, no. 7, pp. 1289–1295, Jul. 1995.
[18] B. Lee, Y. W. Lee, and J. Jung, "Applications of long-period fiber grating pair interferometers for sensors and communications," in *Proc. 15th Annu. Meeting IEEE LEOS*, Nov. 2002, pp. 171–172, paper TuE1.
[19] M. L. Dennis, M. A. Putnam, J. U. Kang, T.-E. Tsai, I. N. Duling, and E. J. Friebele, "Grating sensor array demodulation by use of a passively mode-locked fiber laser," *Opt. Lett.*, vol. 22, no. 17, pp. 1362–1364, Sep. 1997.
[20] P. V. Kelkar, F. Coppinger, A. S. Bhushan, and B. Jalali, "Time-domain optical sensing," *Electron. Lett.*, vol. 35, no. 19, pp. 1661–1662, Sep. 1999.
[21] H. Y. Fu, H. L. Liu, X. Dong, H. Y. Tam, P. K. A. Wai, and C. Lu, "High-speed fibre Bragg grating sensor interrogation using dispersion-compensation fibre," *Electron. Lett.*, vol. 44, no. 10, pp. 618–619, May 2008.
[22] H. Xia, C. Wang, S. Blais, and J. Yao, "Ultrafast and precise interrogation of fiber Bragg grating sensor based on wavelength-to-time mapping incorporating higher order dispersion," *J. Lightw. Technol.*, vol. 28, no. 3, pp. 254–261, Feb. 1, 2010.
[23] C. Wang and J. Yao, "Ultrafast and ultrahigh-resolution interrogation of a fiber Bragg grating sensor based on interferometric temporal spectroscopy," *J. Lightw. Technol.*, vol. 29, no. 19, pp. 2927–2933, Oct. 1, 2011.
[24] W. Liu, M. Li, C. Wang, and J. Yao, "Real-time interrogation of a linearly chirped fiber Bragg grating sensor based on chirped pulse compression with improved resolution and signal-to-noise ratio," *J. Lightw. Technol.*, vol. 29, no. 9, pp. 1239–1247, May 1, 2011.
[25] F. Coppinger, A. S. Bhushan, and B. Jalali, "Photonic time stretch and its application to analog-to-digital conversion," *IEEE Trans. Microw. Theory Techn.*, vol. 47, no. 7, pp. 1309–1314, Jul. 1999.
[26] X. Li, W. Zou, and J. Chen, "41.9 fs hybridly mode-locked Er-doped fiber laser at 212 MHz repetition rate," *Opt. Lett.*, vol. 39, no. 6, pp. 1553–1556, Mar. 2014.
[27] X. Li, W. Zou, G. Yang, and J. Chen, "Direct generation of 148 nm and 44.6 fs pulses in an Erbium-doped fiber laser," *IEEE Photon. Technol. Lett.*, vol. 27, no. 1, pp. 93–96, Jan. 1, 2015.